SYNTHESIS AND OPTICAL CHARACTERIZATION OF $Eu(TTA)_3(Ph_3PO)_2$

O. T. Bordian[1], V. I. Verlan[1*], M. S. Iovu[1], I. P. Culeac[1], V. E. Zubarev[2], D. E. Bojin[3], and M. Enachescu[3]

[1]Institute of Applied Physics, Academy of Sciences of Moldova, Academiei str. 5, Chisinau, MD-2028 Republic of Moldova
[2]Institute of Chemistry of the Academy of Sciences of Moldova, Academiei str. 3, Chisinau, MD-2028 Republic of Moldova
[3]CSSNT, University Politehnica of Bucharest, Nr 313 Splaiul Independentei, sector 6, Bucharest, RO-060042, Romania
*E-mail *vverlan@gmail.com*

(Received October 15, 2015)

Abstract

Coordination compound tris(thenoyltrifluoroacetonato)bis(triphenylphosphine oxide) europium(III) $Eu(TTA)_3(Ph_3PO)_2$, where TTA is the thenoyltrifluoroacetonate monoanion ($C_8H_5F_3O_2S$), Ph_3PO is triphenylphosphinoxide (TPPO), is synthesized. Solutions with different molar ratios of $Eu(TTA)_3(Ph_3PO)_2$ and thin film samples is characterized by optical transmission and photoluminescence (PL) spectroscopy. The displacement of the absorption threshold to infrared is observed with increasing coordination material concentration in solutions. PL emission at T = 300 K in the solutions and the bulk material is detected as specific bands of the internal transitions in the *4f* shell of the Eu^{3+} ion $^5D_0 \rightarrow {}^7F_i$ (i = 0,1,2,3 and 4) centered at 537, 578, 615, 650, and 702 nm. The dominant PL band is positioned at 615 nm with the FWHM less than 10 nm, and this band is attributed to the transition $^5D_0 \rightarrow {}^7F_2$.

1. Introduction

Coordination compounds of rare earth metals are excellent materials for a new generation of light emitting devices with high efficiency, easy color tuning, temperature insensitivity, and high stability [1]. Owing to excellent PL properties, these compounds and solutions thereof are widely used in medicine, solar cells, optical amplifiers, etc. For application in visible spectrum, compounds with europium (Eu^{3+}) and terbium (Tb^{3+}) ions are more frequently used. Improvement of the luminescence properties of the compounds depends on the type of ligands used for surrounding of the rare earth ions. For example, in this case, photoactive complexes of organic compounds of lanthanides may be used, such as the trivalent ion of Eu^{3+} chelated with β-diketonates, or the cyclic ligands of carboxylate, when the coordination number of Eu^{3+} varies in a range of 6–9 [2]. The efforts of the researchers have been oriented towards achieving compatible coordinated surrounding of the Eu^{3+} ion in order to improve the luminescence efficiency and prepare a final stable compound.

Spectroscopic studies of rare earth organic compounds and applications of the technology associated with effective luminescence with the half-width of the luminescence (FWHM) less than 10 nm in the visible and near-infrared are of special interest. An advantage of application of coordination compounds of rare earth ions with β-diketonates and ligands is based on the so-called "antenna" effect, or the transfer of excitation energy from outside of the system of Eu^{3+} ion towards

the energy levels thereof [2–5]. In this case, the population of upper energy levels increases with subsequent transition to ground states. Strong luminescence of lanthanide complexes determines the application as excitation energy transfer additives in polymer materials in optoelectronics, biology, power industry, and medicine.

Over the last years, attention has been focused on studying the structure and luminescent properties of europium complexes with different acceptor diketonates and donor ligands [6]. The use of these diketonetes and donor ligands gives the possibility to modify the symmetry of the structure around the rare earth ion and thus allow transitions *4f* → *4f*, which are forbidden in the symmetric spherical surround of the Eu^{3+} ion, making luminescence uninterrupted without accumulation or loss of energy, and the application of dissolution of coordination compounds in different solvents, both polar and nonpolar.

2. Experimental

The synthesis of coordination compound of tris(thenoyltrifluoroacetonato)bis(triphenylphosphine oxide)europium(III) ($Eu(TTA)_3(Ph_3PO)_2$) was conducted similar to the scheme described in [7] with some modifications. All chemicals were purchased from Aldrich Chemical Company.

Synthesis: 0.66 g (3 mmole) of thenoyltrifluoroacetone (TTA) and 0.56 g (2 mmole) of triphenylphosphine oxide (TPPO) were dissolved in 10 mL of warm 96% ethanol and 3 mL of a 1 N sodium hydroxide solution was added. The mixture was stirred, while 1 mmole of europium chloride in 5 mL of water was added dropwise. A light pink precipitate was immediately formed. The precipitate was filtered off, washed with small portions of ethanol and diethyl ether, dried thoroughly in air, and the solid of the complex was obtained. The yield was 0.68 g.

For $C_{60}H_{42}F_9EuO_8P_2S_3$ calcd, %: C = 52.53; H = 3.09.

Found, %: C = 52.37; 52.28; H = 3.18; 2.98.

Structural formula of $Eu(TTA)_3(Ph_3PO)_2$ ($C_{60}H_{42}F_9EuO_8P_2S_3$) [8] is represented in Fig. 1.

Solutions of $Eu(TTA)_3(Ph_3PO)_2$ in toluene were prepared with different ratios of weight concentrations, %: 0.017, 0.053, 0.16, 0.5, 1.5, 4.5, and 13.6.

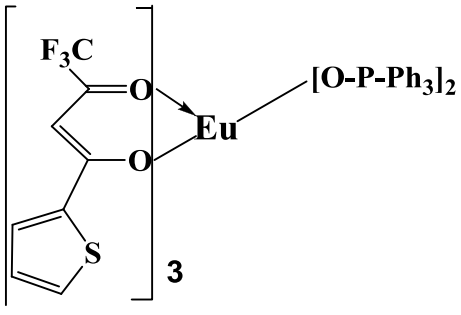

Fig. 1. Structural formula of $C_{60}H_{42}F_9EuO_8P_2S_3$.

Microscopic investigations of the morphology of the surface were carried out with a TEM EM 410 transmission electron microscope. PL spectra excited by a N_2-laser (λ = 337 nm) or a diode laser (λ = 405 nm) were measured using a set-up based on an MDR-23 monochromator connected to a PC. For optical transmission investigations, a Specord UV/VIS (300–800 nm) CARL ZEISS Jena unit was used. All the measurements were performed at room temperature.

The Fourier transform infrared (FTIR) spectra were measured on a Perkin-Elmer infrared spectrophotometer using the KBr pellet technique.

3. Experimental results

TEM examination of solutions of the powder samples in a toluene solution reveals that $Eu(TTA)_3(Ph_3PO)_2$ complexes are dispersed homogenously without any phase separation. According to TEM, the dimensions of the $Eu(TTA)_3(Ph_3PO)_2$ particles in the thin films and in the solutions are in a range of 20–30 nm.

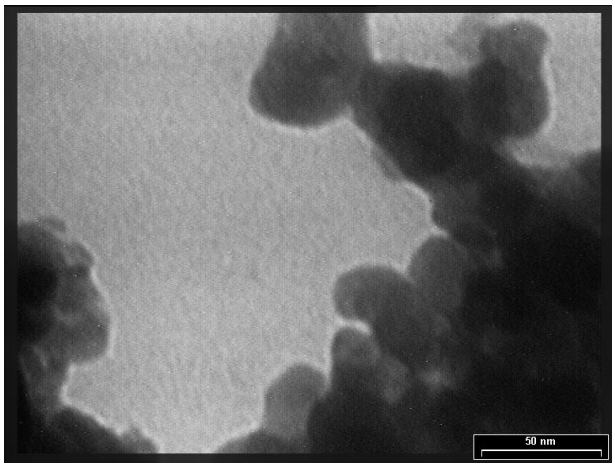

Fig. 2. TEM image showing the distribution of $Eu(TTA)_3(Ph_3PO)_2$ particles.

Figure 3 illustrates optical transmission spectra of the solution of $Eu(TTA)_3(Ph_3PO)_2$ particles in toluene at different concentrations. The absorption threshold in the domain of 320–400 nm can be clearly seen; with an increase in the $Eu(TTA)_3(Ph_3PO)_2$ concentration in the solution, it is shifted towards the infrared. Figure 3 shows the transmission spectrum of the thin film samples deposited on a quartz substrate. Transmission spectra $T(\lambda)$ of the solutions with different $Eu(TTA)_3(Ph_3PO)_2$ concentrations in the ultraviolet (UV) clearly show absorption bands peaking at 3.39, 4.56, 5.37, and 6.14 eV. A sharp absorption threshold is present at all concentrations of the $Eu(TTA)_3(Ph_3PO)_2$ coordinated compounds in a spectral range of 370-380 nm.

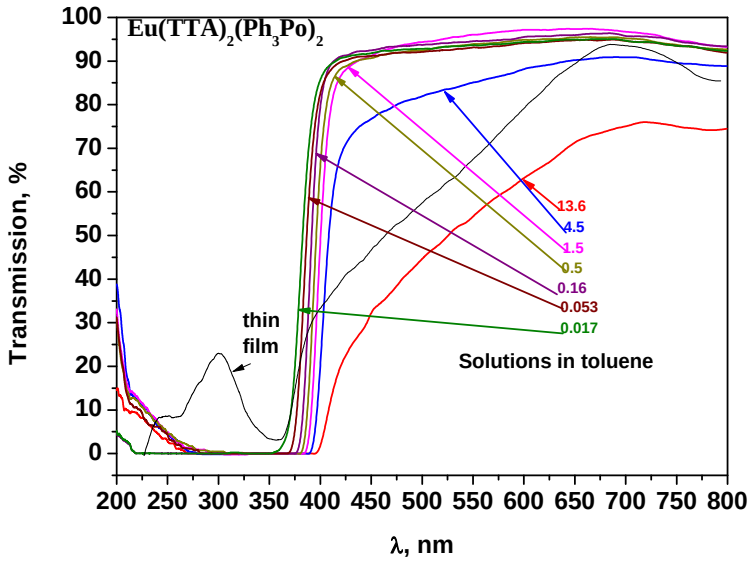

Fig. 3. Transmission spectra of the solutions and the thin layers deposited on quartz substrates at different $Eu(TTA)_3(Ph_3PO)_2$ concentrations at room temperature.

Absorption spectra $\alpha(\lambda)$ are calculated from transmission spectra $T(\lambda)$ through the relation ship $D(\lambda) = \alpha(\lambda)cl = - lnT$, where D is the optical density, c is the molar concentration of $Eu(TTA)_3(Ph_3PO)_2$ in solution, l is the thickness of the measuring quartz cuvette, and α is the absorption coefficient. The band-gap energy of the NC, ΔE_{HL} = LUMO – HOMO, (where HOMO is the energy of the highest occupied molecular orbital, and LUMO is the energy of the lowest unoccupied molecular orbital), which is obtained from 80% of the absorption threshold $T(\lambda)$, are in a range of 3.14–3.16 eV.

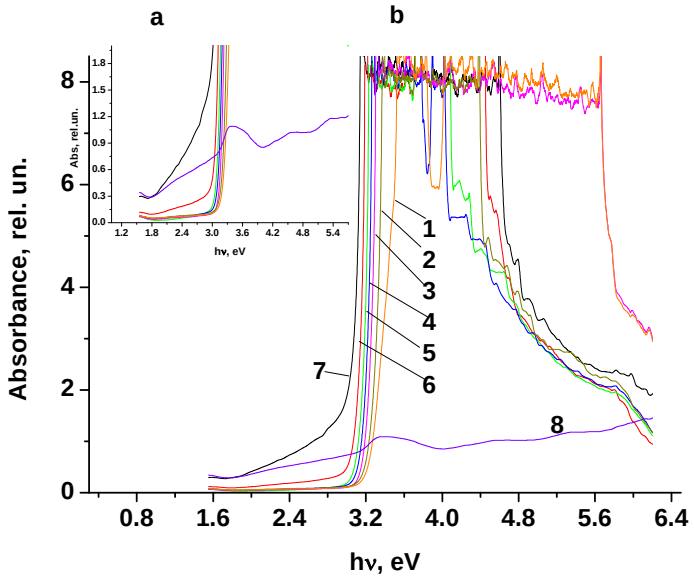

Fig. 4. Absorption spectra of the solutions and the thin layer on a quartz substrate at different $Eu(TTA)_3(Ph_3PO)_2$ concentrations in solution at room temperature, wt %: (*1*) 4.5, (*2*) 1.5, (*3*) 0.5, (*4*) 0.16, (*5*) 0.053, (*6*) 0.017; (*7*) the thin film of $Eu(TTA)_3(Ph_3PO)_2$; *(8)* thin layer $Eu(TTA)_3(Ph_3PO)_2$/PEPC deposited on quartz substrate.

The difference in the absorption onset of the solutions with different $Eu(TTA)_3(Ph_3PO)_2$ concentrations is mostly determined by the difference in the particles size which probably increases with increasing concentration. This fact is generally attributed to particles aggregation; it is confirmed by the registered TEM images.

Figure 5 illustrates the PL spectra of the $Eu(TTA)_3(Ph_3PO)_2$ solution in toluene under excitation of an N_2-laser beam. The registered PL bands correspond to the radiative transitions between the energy *4f*-levels of the Eu^{3+} ions and are centered at 537, 578, 615, 650, and 702 nm and can be attributed to the spin forbidden $4f \rightarrow 4f$ transitions $^5D_0 \rightarrow {}^7F_i$ (i = 0, 1, 2, 3, 4). The most effective luminescence at room temperature has a maximum at 615 nm, which is about 20 times higher than that of other PL bands, and its half-width is less than 10 nm. The PL intensity of almost monotonically increases with increasing compound concentration in the solution; this feature is characteristic of all thin film samples at room temperature.

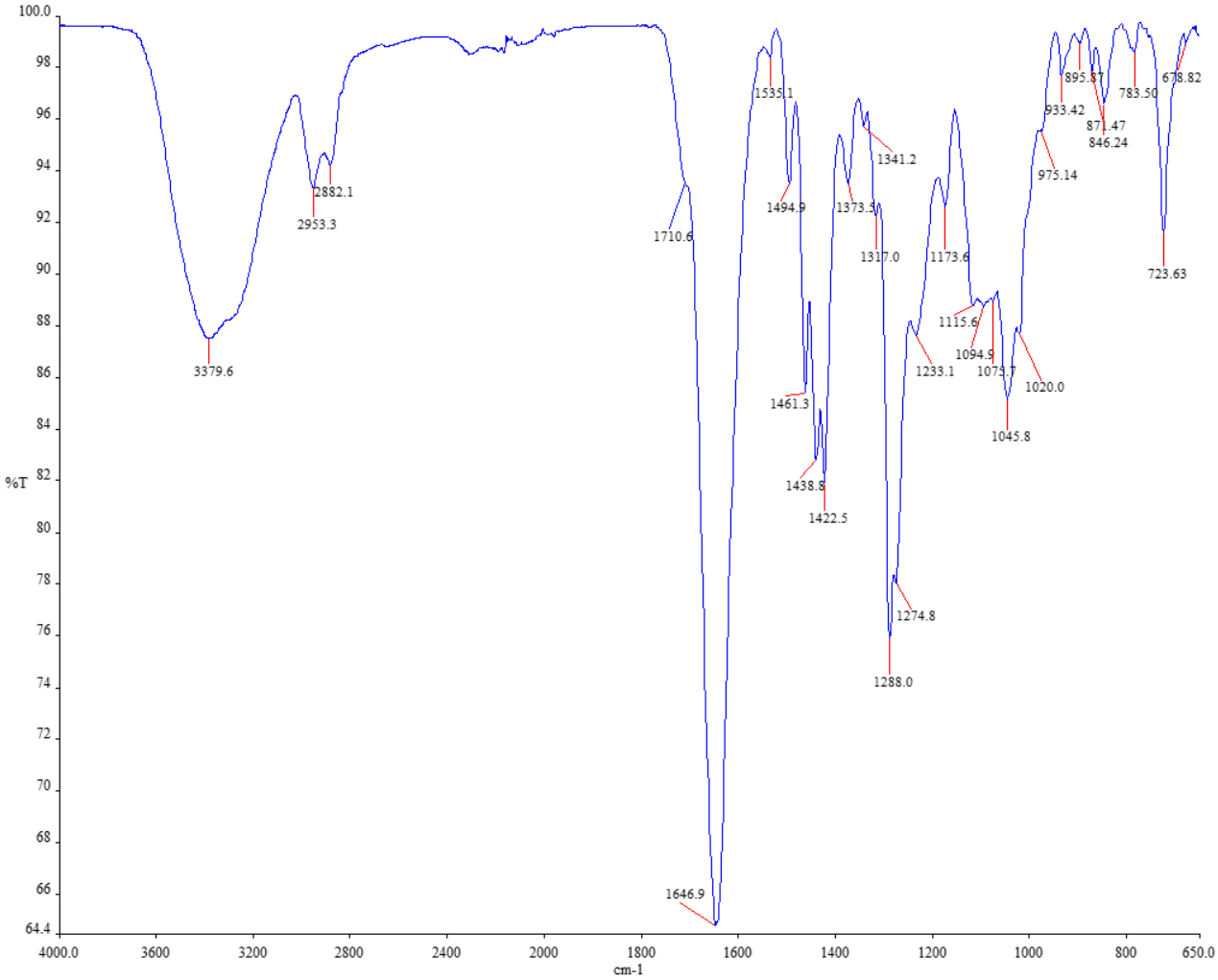

Fig. 5. IR transmission spectra of the thin film samples deposited on quartz substrates at different $Eu(TTA)_3(Ph_3PO)_2$ concentrations at room temperature.

Table 1. Positions of the IR absorption peaks (cm^{-1}) for the $Eu(TTA)_3(Ph_3PO)_2$ powder samples (cm^{-1})

λ, cm^{-1}	λ, cm^{-1}	λ, cm^{-1}	λ, cm^{-1}	λ, cm^{-1}
3379.6	1494.9	1317.0	1094.9	895.9
2953.3	1461.3	1288.0	1075.7	871.5
2882.1	1438.8	1274.8	1045.8	846.2
1710.6	1422.5	1233.1	1020.0	783.5
1646.9	1373.5	1173.4	975.1	723.8
1535.1	1341.2	1115.6	933.4	671.8

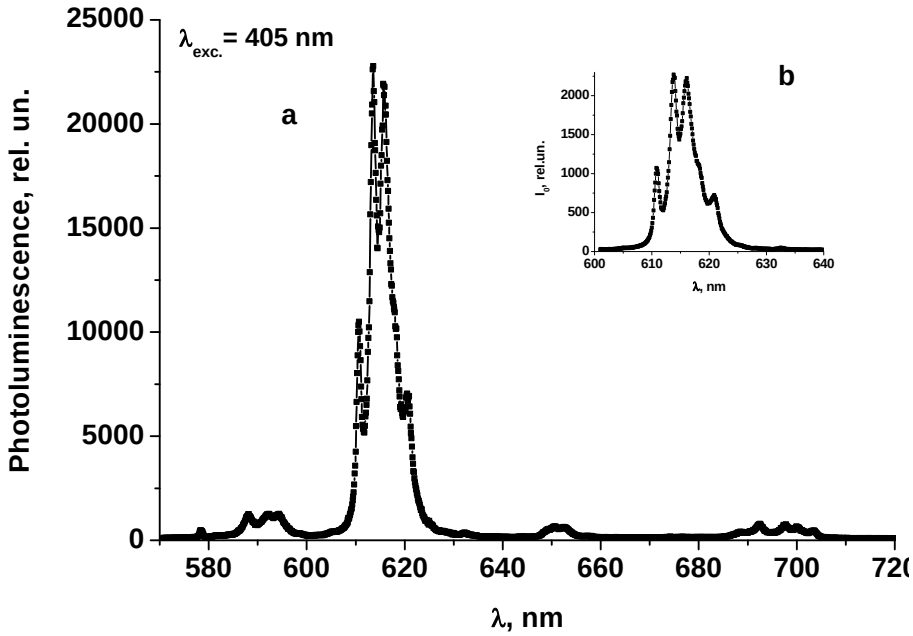

a), b)

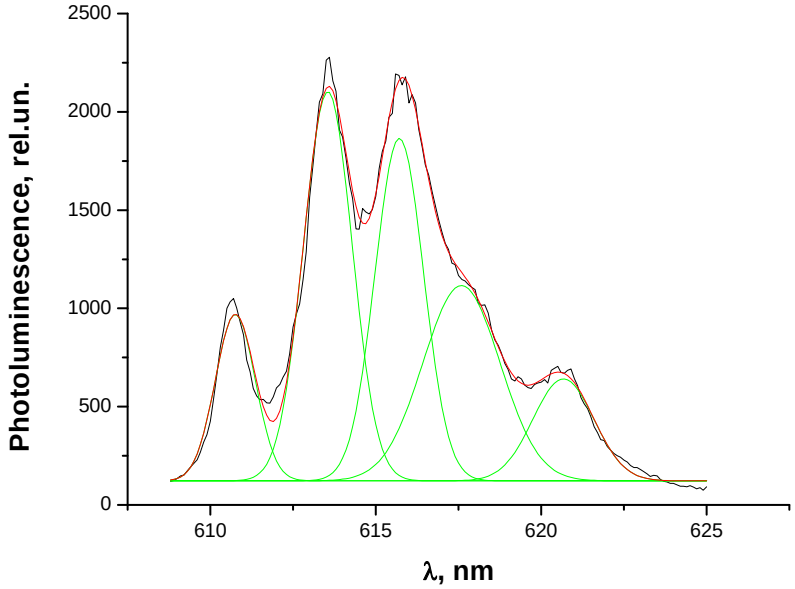

c)

Fig. 6. PL spectra at room temperature of thin sample layers of the $Eu(TTA)_3(Ph_3PO)_2$ complex: (a) the total spectrum; (b) PL graphic in the interval (600 – 640 nm) (c) the detailed spectrum of main maximum.

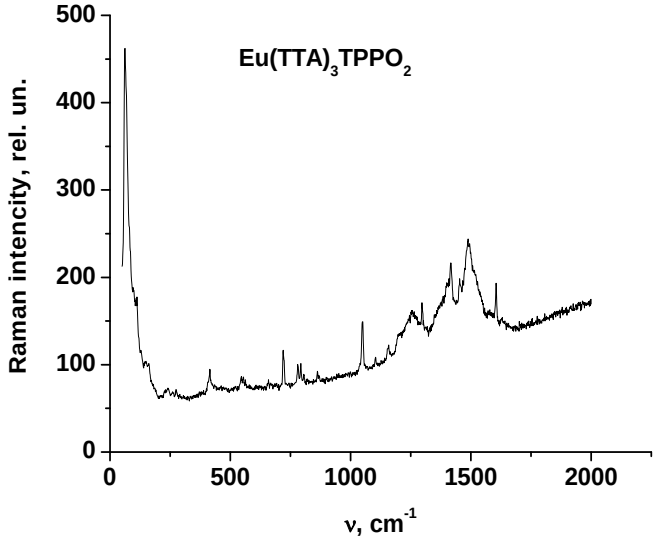

Fig. 7. Raman spectrum of the $Eu(TTA)_3(Ph_3PO)_2$ powder.

Table 2. The position of maxima of Raman interactions in the $Eu(TTA)_3(Ph_3PO)$ powder

λ, cm^{-1}	λ, cm^{-1}	λ, cm^{-1}	λ, cm^{-1}
69.5	667.2	1108.6	1420.0
156.7	723.2	1164.7	1488.4
237.6	791.7	1208.3	1575.5
418.1	870.0	1258.1	1606.7
548.9	1046.9	1295.4	

4. Discussion

There is a rather weak and broad band at 578.5 nm associated with the $^5D_0 \rightarrow {}^7F_0$ transition. Based on selection rules, the band at 594 nm is attributed to the $^5D_0 \rightarrow {}^7F_1$ parity-allowed magnetic dipole transition, which is independent of the surroundings symmetry. The $^5D_0 \text{—>} {}^7F_2$ transitions are allowed electrical-dipole transitions. The most intensive band around 614 nm belongs to the $^5D_0 \text{-}\rightarrow {}^7F_2$ transition, which is hyper-sensitive to the symmetry of the crystal field surrounding the Eu ion, and will be relatively strong if the surroundings symmetry is low. In this respect, it is known that the ratio of emission intensities $R = I(^5D_0 \rightarrow {}^7F_2)/I(^5D_0 \rightarrow {}^7F_1)$ is an asymmetry parameter for the Eu^{3+} sites and a measure of the extent of Eu^{3+} interaction with surrounding ligands, indicating on the environment of the Eu^{3+} ion.

In Fig. 5, one can clearly observe two well developed emission lines centered at 652 and 702 nm that originate from $^5D_0 \rightarrow {}^7F_3$ and $^5Do \rightarrow {}^7F_4$ transitions, respectively. It is also important to note that crystallized particles exhibit much stronger luminescence emission.

PL spectra characterize the efficiency of energy transfer from the LUMO energy levels of chelates and ligands of the compound to the energetic levels of Eu^{3+} ion of 4f level: $^5D_0 \rightarrow {}^7F_i$. HOMO and LUMO levels of the $Eu(TTA)_3(Ph_3PO)_2$ complex are found to be situated between

levels *S* and *T* of the ligands; this case is similar to doping of semiconductors.

The registered PL emission spectra are similar to those of the respective $Eu(TTA)_3Phen$ complex [1–2], and half widths of the strongest PL band are found to be less than 10 nm. In the case of this band, $Eu(TTA)_3(Ph_3PO)_2$ exhibits the most high fluorescence intensity and color purity. In this case, the PL displays a bright and narrow Eu^{3+} ion emission, which is due to the so-called "antenna" effect, defined as a light conversion process via an absorption energy transfer-emission sequence, involving distinct photon absorption by a ligand and subsequent energy transfer to Eu^{3+} ions and final photon emission. The PL experimental data can be explained taking into account the surrounding environment of the Eu^{3+} ion. For the Eu complex, the intensity of optical transitions ${}^5D_0 \rightarrow {}^7F_i$ (i = 0, 1, 2, 3, 4) increases with increasing $Eu(TTA)_3(Ph_3PO)_2$ concentration in the solutions (Fig. 8).

The difference of the PL spectra of the $Eu(TTA)_3(Ph_3PO)_2$ complex in different solutions can be interpreted as follows. If complexes of particles are dissolved in solutions, the molecular motion is restricted and the stretching and bond vibrations are weakened by the solutions, both of which decrease the nonradiative transition. These results indicate that the solutions cannot provide a relatively stable environment for lanthanide complexes.

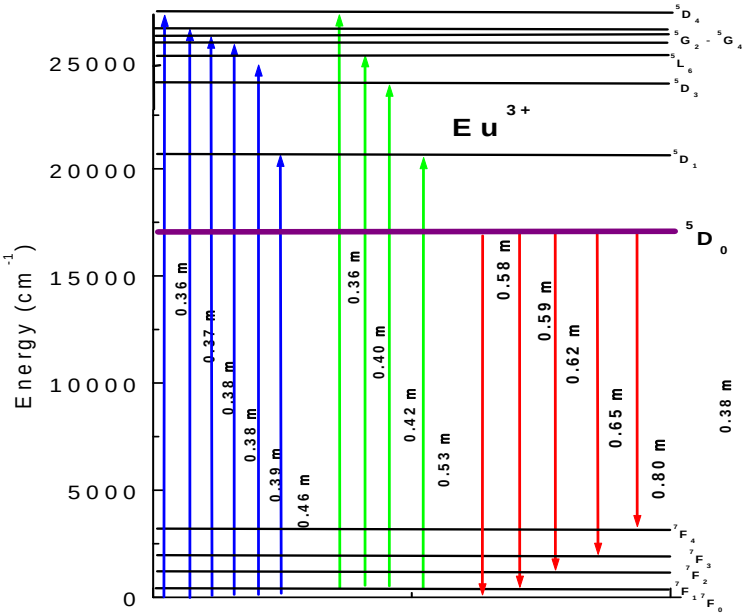

Fig. 8. Illustration of optical transitions in the 4f shell of the Eu^{3+} ion related to absorption (blue and green arrows) and emission processes (red arrows).

We can suppose that the interaction of macromolecular ligands and the Eu^{3+} ion in solutions leads to the partial formation of coordinated unsaturated complexes and ionic aggregates resulting in the luminescence quenching. From the PL spectra (Fig. 6), we can suppose a low local symmetry of the ligand field of the Eu^{3+} ion owing to the observed line transition ${}^5D_0 \rightarrow {}^7F_0$, which is forbidden under the high symmetry of the luminescence centre. The intensity of the transition ${}^5D_0 \rightarrow {}^7F_0$ is comparable with intensities of ${}^5D_0 \rightarrow {}^7F_1$, indicating also a significant asymmetry around of the rare-earth ions. The presence of splitting of all transition lines ${}^5D_0 \rightarrow {}^7F_i$ on five components indicates also the absence of an axial symmetry of the inner coordination sphere of the central Eu^{3+} ion [1].

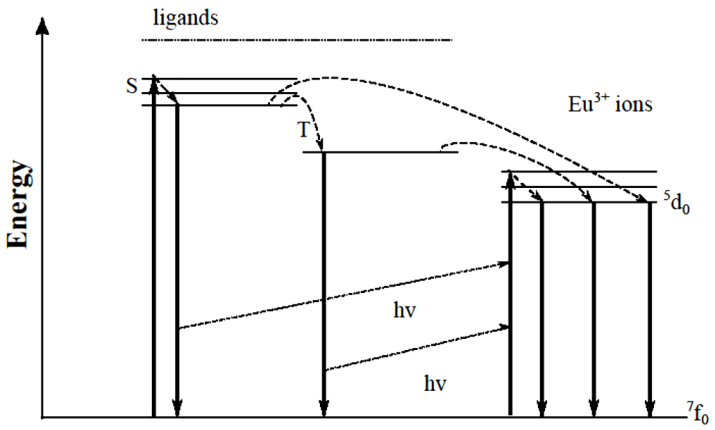

Fig. 9. Illustration of the mechanism of energy transfer and PL in the $Eu(TTA)_3(Ph_3PO)_2$ solution in toluene.

5. Conclusions

A PL solution based on the $Eu(TTA)_3(Ph_3PO)_2$ coordination compound has been synthesized and characterized by PL and UV-Vis absorption spectroscopy. From the transmission spectra, we have identified the basic absorption bands with maximums centered at 3.8, 4.5, and 4.8 eV in the UV. The absorption threshold has been estimated as E_{LH} = 3.15 eV. It is slightly shifted to *IR* with increasing $Eu(TTA)_3(Ph_3PO)_2$ concentration in the solution.

The PL properties can be attributed to the internal *4f* transition of the Eu^{3+} ion $^5D_0 \rightarrow {}^7F_i$ (i = 0, 1, 2, 3, 4). The FWHM of the PL band at 615 nm is less than 10 nm; this fact suggests that the $Eu(TTA)_3(Ph_3PO)_2$ compound exhibits high emission and color purity. Each maximum of the PL band is split in five components.

The positive effect of TTA and TPPO ligands on the coordinative environment of the Eu^{3+} ions has been found. A possible method for improving the fluorescence efficiency of $Eu(TTA)_3(Ph_3PO)_2$ is the energy transfer from *S* and *T* of ligands levels to internal *4f* levels of the Eu^{3+} ion. This research may provide a new method for designing and studying the crystal structure and symmetry of the luminescent $Eu(TTA)_3(Ph_3PO)_2$ hybrid material for the preparation of UV excited devices; further studies are currently underway.

Acknowledgments. This work was supported by the Romanian Executive Agency for Higher Education, Research, Development and Innovation Funding (UEFISCDI) through the program PN-686/ 22.04.2013, by the Supreme Council for Science and Technological Development (CSŞDT) of the Academy of Sciences of Moldova of numbers 15.817.02.03A and research grants 11.817.05.03A, 13.820.05.15/RoF and 14.819.02.20A.

References

[1] Koen Binnemans, Rare-Earth Beta-Diketonates, in Handbook on the Physics and Chemistry of Rare Earths, ed. by K. A. Gschneidner, Jr., J.-C. G. Bünzli and V. K. Pecharsky, Elsevier, vol. 35, ch. 225, pp. 107–271, 2005.

[2] M. S. Iovu, A. M. Andriesh, S. A. Buzurniuc, V. I. Verlan, M. I. Caraman, and V. E. Zubarev, J. Optoelelectron. Adv. Mater. 10 (4), 841, (2008).

[3] A. Andriesh, S. Buzurniuc, V. Verlan, M. I. Caraman, S. Robu, and N. Barba, J. Optoelelectron. Adv. Mater. 10, 353, (2008).
[4] M. S. Iovu, A. M. Andriesh, S. A. Buzurniuc, V. I. Verlan, C. I. Turta, V. E. Zubareva, and M. I. Caraman, J. Non-Cryst. Solids 355, 1890, (2009).
[5] M. S. Iovu, S. A. Buzurniuc, V. I. Verlan, I. P. Culeac, and Yu. H. Nistor, Advanced Topics in Optoelectronics, Microelectronics, and Nanotechnologies IV, Ed. by P. Schiopu, C. Panait, G. Caruntu, and A. Manea, Proc. SPIE 7297, 729703, (2009).
[6] V. A. Batyreva, A. I. German, and V. V. Serebrenikov, Synthesis of Rare Earth Compounds, Part 2, Tomsk, University of Tomsk, 1986, p. 121.
[7] V. I. Verlan, M. S. Iovu, I. Culeac, Y. Nistor, C. I. Turta, V. E. Zubareva, and S. Buzurniuc, J. Non-Cryst. Solids 357, 1004, (2011).
[8] Cambridge Structural Database. www.ccdc.cam.ac.uk/data_request/cif.